DOI: 10.1002/chem.200801025

Facile High-Yield Synthesis of Polyaniline Nanosticks with Intrinsic Stability and Electrical Conductivity

Xin-Gui Li,*[a, b] Ang Li,[a] and Mei-Rong Huang*[a, b]

Abstract: Chemical oxidative polymerization at 15 °C was used for the simple and productive synthesis of polyaniline (PAN) nanosticks. The effect of polymerization media on the yield, size, stability, and electrical conductivity of the PAN nanosticks was studied by changing the concentration and nature of the acid medium and oxidant and by introducing organic solvent. Molecular and supramolecular structure, size, and size distribution of the PAN nanosticks were characterized by UV/Vis and IR spectroscopy, X-ray diffraction, laser particle-size analysis, and transmission electron microscopy. Introduction of organic solvent is advantageous for enhancing the yield of PAN nanosticks but disadvantageous for formation of PAN nanosticks with small size and high conductivity. The concentration and nature of the acid medium have a major influence on the polymerization yield and conductivity of the nanosized PAN. The average diameter and length of PAN nanosticks produced with 2 M HNO_3 and 0.5 M H_2SO_4 as acid media are about 40 and 300 nm, respectively. The PAN nanosticks obtained in an optimal medium (i.e., 2 M HNO_3) exhibit the highest conductivity of 2.23 S cm^{-1} and the highest yield of 80.7 %. A mechanism of formation of nanosticks instead of nanoparticles is proposed. Nanocomposite films of the PAN nanosticks with poly(vinyl alcohol) show a low percolation threshold of 0.2 wt %, at which the film retains almost the same transparency and strength as pure poly(vinyl alcohol) but 262 000 times the conductivity of pure poly(vinyl alcohol) film. The present synthesis of PAN nanosticks requires no external stabilizer and provides a facile and direct route for fabrication of PAN nanosticks with high yield, controllable size, intrinsic self-stability, strong redispersibility, high purity, and optimizable conductivity.

Keywords: conducting materials · nanostructures · polymerization · polymers · semiconductors

Introduction

The conducting polymer polyaniline (PAN) is very attractive due to its inexpensive monomer, ease of synthesis, widely controllable conductivity[1] and excellent environmental stability. Thus, PAN has superior suitability for commercial application than non-intrinsically conducting polymers that are merely physical mixtures of an insulating polymer with conducting materials such as carbon black and graphite. Nanomaterials have novel chemical and physical properties because of the small size and quantum effect of the nanostructures. Recently, one-dimensional PAN nanostructures such as nanowires, nanosticks, and nanotubes have attracted much attention due to properties such as intrinsic electrical conductivity and special nanoeffects, and the associated promising applications in nanodevices and other important fields.[2]

Template, electrochemical, and even physical methods involving electrospinning and mechanical stretching[3–5] are used to prepare nanostructured PAN. Examples of the fabrication of one-dimensional nanosized PAN include PAN nanofibers by potential cycling[6] and interfacial polymerization,[7] Fe_3O_4 nanoparticles containing PAN nanotubes by an ultrasonic technique,[8] and submicrometer PAN/nano-ZnO composite fibers.[9] However, the complex preparation and/or imperfect performance of the nanosized PAN products restricted the extent of practical applications of these methods. Copolymerization has been used to prepare nanostructured aniline copolymers by a template-free method that introduces functional groups such as SO_3^- in comonomers.[10–11] Electrically conductive copolymer nanoparticles

[a] Prof. Dr. X.-G. Li, A. Li, Prof. M.-R. Huang
Institute of Materials Chemistry
College of Materials Science & Engineering
Tongji University, 1239 Si-Ping Road, Shanghai 200092 (China)
Fax: (+86) 21-65980524
E-mail: adamxgli@yahoo.com
huangmeirong@tongji.edu.cn

[b] Prof. Dr. X.-G. Li, Prof. M.-R. Huang
Key Laboratory of Molecular Engineering of Polymers
Fudan University
Shanghai 200433 (China)

were thus prepared, but the conductivity of the copolymer particles was not markedly improved, and the cost of the functionalized comonomer was relatively high. It seems that some inherent problems regarding nanosized PAN prepared by traditional emulsion and dispersion polymerization remain to be solved, such as low self-stability, complicated preparation process, small synthesis scale, and impure composition. Recently, two facile template-free approaches using interfacial and rapidly mixed polymerization to avoid secondary growth for the synthesis of the PAN nanofibers in an aqueous system have been reported.[12] The size and morphology of the nanofiber products are good, but the yield of the PAN nanofibers, which is an important parameter for estimating the practical value of the method in potential applications, was not elaborated so far.

In this study, we used traditional chemical oxidative polymerization in the absence of any external additives or internal ionic side groups to directly and facilely synthesize one-dimensional PAN nanosticks with inherent self-stability (i.e., stable dispersion without visible precipitation in pure water in the absence of stabilizers over a certain period of time), high preparation yield, and superior and stable conductivity. The effect of polymerization media on the yield, molecular and supramolecular structure, morphology, and properties of the nanosticks was systematically investigated. A template-free method to effectively prepare PAN nanosticks was developed.

Results and Discussion

Synthesis of PAN nanosticks: Ammonium persulfate as oxidant was added dropwise to a solution of aniline (AN) monomer in aqueous HNO_3 to synthesize the PAN nanosticks (Scheme 1). The concentration and nature of the acid medium were varied to study their effects on the rate and yield of polymerization (Figure 1). When the acid concentration is higher than 0.1 M, a light blue PAN is generated in about 10 min and the polymerization rate becomes increasingly faster as the acid concentration is increased from 0.1 to 1.0 M. At an acid concentration higher than 1.0 M, the polymerization rate becomes much higher due to much faster chain initiation. Chocolate-brown oligomers are observed when pure water is used as polymerization medium, because sufficient H^+ is necessary for the oxidant to oxidize AN and then initiate oxidative polymerization.[13a]

Various factors influence the yield, such as oxidant species, oxidant/monomer ratio, medium, temperature, and method of polymerization.[14] The effects of the concentration and nature of the acid medium were studied at a fixed temperature of 15 °C and a constant oxidant/monomer molar ratio of 1/1. As shown in Figure 1, with increasing HNO_3 concentration from 0 to 2 M, the yield of PAN first showed a minimum and then a maximum. The minimal yield at 0.1 M may be due to the weakest polymerizability of AN at the lowest acid concentration. The slightly higher yield in neutral water than in 0.1–0.5 M acidic media could also be assigned to a different coupling mode, as discussed below. Otherwise, the yield would be even lower in neutral water if the coupling mode were the same. The maximal yield of up to 80.7 % is obtained in 2 M HNO_3. Decreased yield in HNO_3 at the concentrations higher than 2 M is attributed to oxidative degradation of the PAN chains by concentrated HNO_3.[15,16] The polymerization yields in 1 M HNO_3 and 0.5 M H_2SO_4 are nearly the same (up to 79 %) and slightly higher than that in 1 M HCl (Table 1).

The dependence of polymerization yield on the concentration and nature of the protic acid mainly results from the variation in polymerizability of AN in different states (protonated or free neutral) in different acidic media. In strong concentrated acid, AN can simply be oxidized to radical cat-

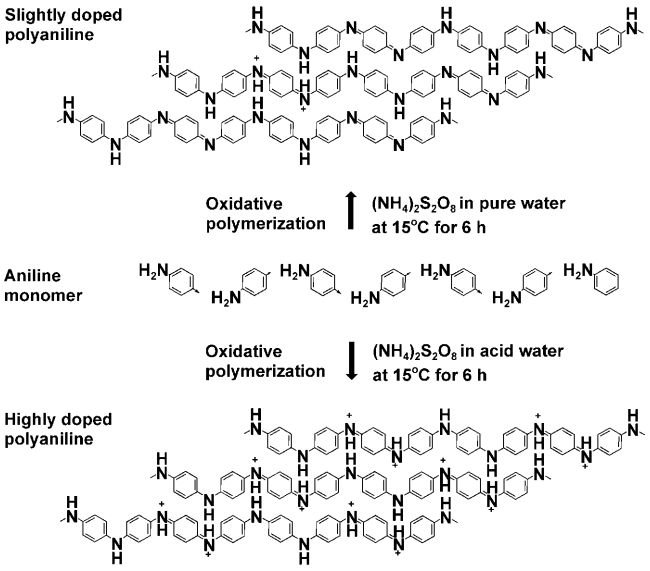

Scheme 1. Chemical oxidative polymerization of aniline and acid-doped chain structures of the PAN particles with $(NH_4)_2S_2O_8$ as oxidant in acid-free pure water (top) and acidic water (bottom) with the same fixed $(NH_4)_2S_2O_8$/aniline monomer molar ratio of 1/1 at 15 °C for 6 h.

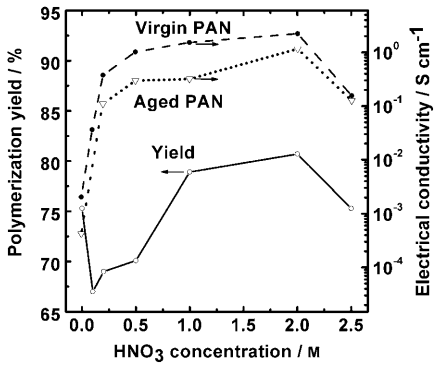

Figure 1. Influence of HNO_3 concentration on the yield of PAN nanosticks with a fixed $(NH_4)_2S_2O_8$/monomer molar ratio of 1/1 at 15 °C for 6 h and on the bulk electrical conductivity of a virgin sample and a sample aged for 480 d at room temperature. The aging time of the PAN synthesized in 2.5 M HNO_3 was 270 days.

Table 1. Synthesis and properties of PAN particles prepared in four polymerization media.

Medium	Yield [%]	λ(UV/Vis) [nm]	$\tilde{\nu}$(quinoid/benzenoid) [cm^{-1}]	D_n [nm]	D_w/D_n	σ [$S\,cm^{-1}$]
H_2O	75.3	601	1592/1498	3871	1.172	2.06×10^{-3}
0.5 M H_2SO_4	79.0	628	1580/1486	106.3	1.412	0.125
1 M HCl	77.4	624	1560/1477	334.5	1.059	0.764
1 M HNO_3	78.9	615	1560/1477	198.6	1.170	1.53

ions that can polymerize by a subsequent coupling step. However, the polymerizability of AN becomes weaker in more dilute acid because the head-to-tail coupling step requires participation of a certain amount of protons.[13b] Therefore, protonation of AN and subsequent head-to-tail coupling in neutral water become more difficult in the absence of H^+. In fact, the N=N character arising from the head-to-head coupling under neutral or basic conditions leads to the formation of chocolate-brown oligomers with poor conjugated structure rather than a dark green polymer with highly π-conjugated structure.[13b,c] The presence of a small number of N=N linkages in PAN has been confirmed by IR spectroscopy. The stability and activity of $(NH_4)_2S_2O_8$ as oxidant may also be dependent on acid concentration. With decreasing acid concentration, an increased number of hydroxyl ions would tend to react with the sulfate radical anions from $(NH_4)_2S_2O_8$.[13d] Consequently, fewer sulfate radicals participate in oxidative polymerization of AN in more dilute acid medium, and the yield is lower.

Introduction of the organic solvent CH_3NO_2 enhances the yield of the PAN particles when $(NH_4)_2S_2O_8$ is used as oxidant (Table 2). This may be due to a slightly different polymerization mechanism caused by the polar organic solvent that results in a head-to-head coupling mode that forms azobenzene units in the polymer with higher yield but lower conductivity (Table 2). This is similar to the oxidative polymerization of AN in neutral (Table 1) or polar acetonitrile/pyridine media.[13b] However, when $FeCl_3$ is used as oxidant instead of $(NH_4)_2S_2O_8$, the yield is lower even if 6 mL of CH_3NO_2 is added. This confirms that $(NH_4)_2S_2O_8$ is a more efficient oxidant for AN polymerization than $FeCl_3$. Apparently, 2 M HNO_3 is the best acid medium for the synthesis of PAN nanosticks with the highest yield and highest conductivity.

Table 2. Synthesis and characterization of PAN particles prepared in 0.5 M HNO_3 containing different amount of CH_3NO_2.

CH_3NO_2 [mL]	Oxidant	Yield [%]	D_n [nm]	D_w/D_n	σ [$S\,cm^{-1}$]
0	$(NH_4)_2S_2O_8$	70.1	292.3	1.109	1.02
3	$(NH_4)_2S_2O_8$	72.0	308.9	1.082	0.249
6	$(NH_4)_2S_2O_8$	75.2	336.2	1.061	0.391
6	$FeCl_3$	64.0	321.4	1.087	5.95×10^{-8}

Macromolecular structure of the PAN particles: The molecular structure of PAN was analyzed by UV/Vis absorption spectroscopy, FTIR absorption spectroscopy, and wide-angle X-ray diffraction (XRD).

UV/Vis spectra: UV/Vis absorption spectra of aqueous dispersions of PAN particles obtained in HNO_3 at different concentrations are shown in Figure 2. The characteristic peaks of PAN at about 350, 430, and 800 nm, are attributed to $\pi\rightarrow\pi^*$, polaron$\rightarrow\pi^*$, and $\pi\rightarrow$polaron transitions, respectively.[17] The result suggests that the PAN dispersions in water have the UV/Vis characteristics of acid-doped PAN solutions in organic solvents, that is, the PAN particles seem to be molecularly dispersed in water despite their aqueous insolubility, and they are nanosized, as discussed below. With increasing HNO_3 concentration the peak at 700–900 nm shifted slightly, and the dispersion of PAN particles obtained in 2 M HNO_3 has a UV/Vis absorbance peak at the shortest wavelength of 730 nm. This is contrast to the variation of the conductivity with acid concentration in Figure 1. This implies that the PAN particles with the highest conductivity, formed in 2 M HNO_3, are the most poorly dispersed in water. This phenomenon has further been proved by the fact that the dispersion of PAN particles obtained in 1 M HNO_3 among four polymerization media exhibits UV/Vis absorbance peak at the shortest wavelength of 747 nm in Figure 3, that is, the PAN particles with the highest conductivity obtained in 1 M HNO_3 are also the most poorly dispersed in water. In both Figures 2 and 3, a sharp peak at about 220 nm is present in every spectrum, but no reports on this band were found so far. Maybe the band at around 220 nm is relevant to the characteristics of the PAN nanostructures with sizes of 20–300 nm.[18]

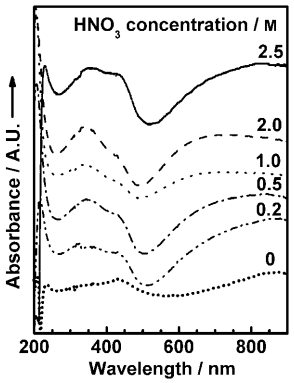

Figure 2. UV/Vis absorption spectra of PAN particle dispersions (in distilled water) prepared in HNO_3 media of six concentrations at a fixed $(NH_4)_2S_2O_8$/aniline molar ratio of 1/1 at 15 °C for 6 h.

Figures 4 and 5 show UV/Vis absorption spectra of solutions of the soluble part of PAN powders in *N*-methylpyrrolidone (NMP). Clearly, these curves are totally different from those discussed above. The band features are similar to those of dedoped PAN in the state of emeraldine base. This

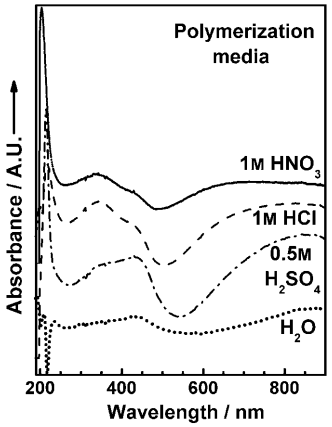

Figure 3. UV/Vis absorption spectra of PAN particle dispersions (in distilled water) prepared in four polymerization media with a fixed $(NH_4)_2S_2O_8$/monomer molar ratio of 1/1 at 15 °C for 6 h.

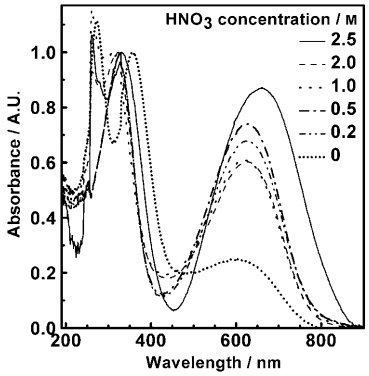

Figure 4. UV/Vis absorption spectra of PAN particle solutions (in NMP and containing a very small amount of insoluble PAN particles) prepared in HNO_3 media with six concentrations with a fixed $(NH_4)_2S_2O_8$/aniline molar ratio of 1/1 at 15 °C for 6 h.

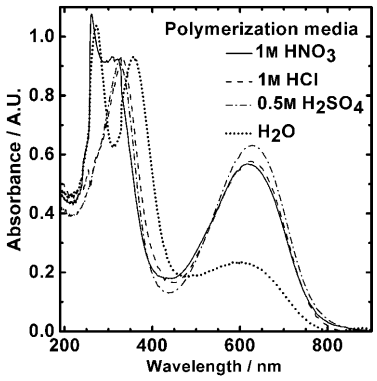

Figure 5. UV/Vis absorption spectra of PAN particle solutions (in NMP and containing a very small amount of insoluble PAN particles) prepared in four polymerization media with a fixed $(NH_4)_2S_2O_8$/monomer molar ratio of 1/1 at 15 °C for 6 h.

could be explained by partially thermal dedoping of the PAN powders during drying at 40 °C for 3 days. The peaks at about 330 and 640 nm are assigned to $\pi \rightarrow \pi^*$ and $n \rightarrow \pi^*$ transitions associated with the excitation of the benzenoid to quinoid rings in the PAN chains.[19] Apparently, the solution of PAN synthesized in pure water displays the weakest band at around 640 nm because it has the most weakly π-conjugated structure, as is shown by its having the lowest conductivity and highest solubility in NMP. The solution of the PAN synthesized in 2 M HNO_3 exhibits the second weakest band at around 640 nm, possibly due to its poorest solubility in NMP, as verified by the presence of the most insoluble particles in solution. Therefore, it is easily understood why the solution of PAN synthesized in 2.5 M HNO_3 exhibits the strongest band at the longest wavelength of around 660 nm because of its second highest solubility in NMP, which is reflected in almost no insoluble particles in the solution. Similarly, the solution of the PAN synthesized in 0.5 M H_2SO_4 of four polymerization media exhibits the strongest band at the longest wavelength of around 628 nm because of its second highest solubility in NMP, as is verified by its second lowest conductivity (Table 1). Clearly, the relationship between UV/Vis band intensity/wavelength and conductivity of the PANs is strongly influenced by their solubility.

FTIR spectra: The FTIR spectra of PANs prepared in four polymerization media (Figure 6) were recorded to analyze the molecular structure and oxidation state of PAN and provide insight into the doping effect of different acids.[20] The wavenumbers of two characteristic absorption peaks are summarized in Table 1. The peak at about 3450 cm^{-1} is due to the N–H stretching vibration. The bands at 1592 and 1498 cm^{-1} are consistent with quinoid and benzenoid ring deformations, respectively.[21] The bands at 1303 and 1150 cm^{-1} are assigned to C–N and C=N stretching vibrations, respectively.[20,22] The strong band at 1150 cm^{-1} was described as an "electronic-like bond" that is considered to be a measure of the degree of delocalization of electrons, that is, a characteristic peak of conducting PAN.[23a] The four IR spectra look similar, but the PAN prepared in acid-free water exhibits a strong peak at 1498 cm^{-1}, a relatively weak peak at 1150 cm^{-1}, and very weak additional peak at 1444 cm^{-1} due to -N=N- stretching that serves as evidence for its low conductivity.[23b] There is no band at 1444 cm^{-1} in

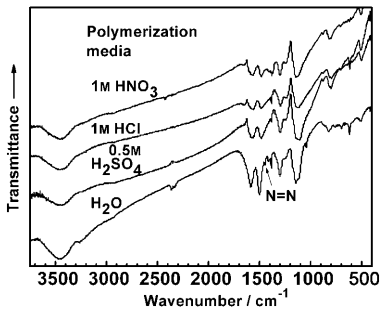

Figure 6. FTIR absorption spectra of PAN prepared in four polymerization media with a fixed $(NH_4)_2S_2O_8$/monomer molar ratio of 1/1 at 15 °C for 6 h.

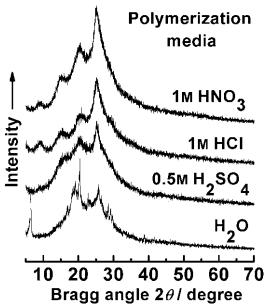

Figure 7. X-ray diffraction patterns for the PAN prepared in four media with fixed $(NH_4)_2S_2O_8$/monomer molar ratio of 1/1 at 15 °C for 6 h.

the other three IR spectra of the PANs synthesized in acidic media. The characteristic peaks due to quinoid and benzenoid ring deformations slightly shift to lower wavenumbers on changing the polymerization medium from H_2O to H_2SO_4 to HCl to HNO_3 (Table 1). This variation coincides with the increase in electrical conductivity. It seems that there is a close relationship between the IR spectra and highly π-conjugated structures of the PANs.

Wide-angle X-ray diffractograms: The wide-angle X-ray diffractograms in Figure 7 reveal that the PAN formed in acid-free water has a different and more highly crystalline structure compared to those prepared in acid media. The three types of PAN particles synthesized in different acid media are all almost amorphous and have similar X-ray diffraction characteristics to one another, because the presence of three bulky acid substituents on the imino groups destroys the regular array of the polymer chains.[24] The similar diffraction features suggest that different doping acids have similar effects on the aggregated structure. The slight differences in diffraction intensity among the three peaks are attributable to the different natures of the anions and the interaction between the anions and the polymer chain. For instance, Cl^- can form a hydrogen bond with an H atom in the PAN backbone chain. Lower crystallinity is also due to higher molecular weight, as was revealed by the more strongly π-conjugated structure (Figure 5) and much higher conductivity (Table 1). Apparently, the higher intensity of the peak at a Bragg angle of 25.7° compared to that at 20.4° can be taken as characteristic for a highly doped PAN.[17,25] However, only PAN particles synthesized in pure water exhibit the strongest and sharpest peak at a Bragg angle of 20.4°, which could be the characteristic of a slightly doped PAN. This result is in good agreement with emeraldine salt doped with acetic acid with lower dissociation constant.[26] Two strong peaks centered at 25.7 and 20.4° may be ascribed to periodicities perpendicular and parallel to the polymer chains, respectively.[27] The peak at 20.4° also represents the characteristic interchain distance of PAN.[28]

Particle size and its distribution: Laser particle-size analysis (LPA) and transmission electron microscopy (TEM) were employed to analyze the polydispersity and observe the morphology and size of the nanostructured PANs prepared in various polymerization media. Figure 8 and 9a show the size and size distribution for PAN particles synthesized in HNO_3 at five different concentrations. The HNO_3 concentration has a significant effect on particle size and polydispersity. The number-average diameter D_n decreases with increasing HNO_3 concentration from 0 to 2 M. In particular,

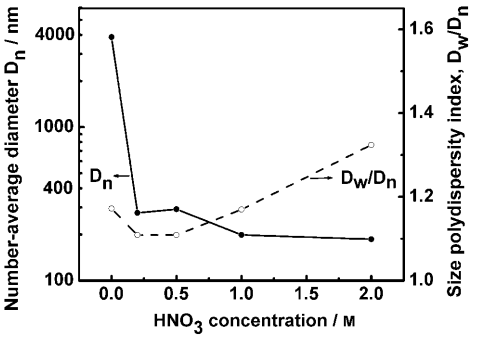

Figure 8. Variation of the number-average diameter D_n and polydispersity index D_w/D_n of PAN particles (in pure water) synthesized in HNO_3 with five different concentrations at 15 °C with a monomer/$(NH_4)_2S_2O_8$ molar ratio of 1/1 for 6 h, determined by laser particle-size analysis (LPA).

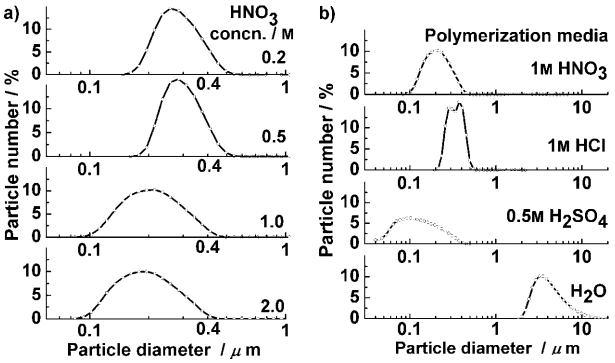

Figure 9. Size distribution of the PAN nanosticks (in pure water) prepared in HNO_3 medium at four concentrations (left) and four media (right) with the same fixed $(NH_4)_2S_2O_8$/aniline molar ratio of 1/1 at 15 °C for 6 h, determined by laser particle-size analysis (LPA).

the PAN particles prepared in 0.2–0.5 M HNO_3 have the smallest polydispersity index (PDI, defined as D_w/D_n, where D_w is weight-average diameter) of 1.109, whereas the PAN particles prepared in 2 M HNO_3 are the smallest with the a D_n value of 186 nm because the particles should be the most highly doped in 2 M HNO_3 (Figure 1), the most highly charged, and thus the most self-stable.

The D_n and D_w/D_n of PAN particles prepared in four polymerization media (Figure 9b and Table 1) indicate that the concentration and nature of the acid medium have a remarkable effect. The PAN particles synthesized in H_2SO_4 are the smallest but the most widely distributed, while the PAN particles obtained in HNO_3 have the second smallest D_n and the second smallest D_w/D_n. Note that the PAN particles formed in acid-free pure water have the largest D_n because of the absence of positively charged PAN chains from acid (Scheme 1). Notably, the PAN particles produced in HCl have the smallest D_w/D_n possibly due to the smallest size of the Cl^- anion, which is conversely confirmed by the largest D_w/D_n when H_2SO_4 with the largest anion is used as acid medium. Obviously, the size distribution of PAN nanoparticles fabricated in HCl is extremely narrow and even more uniform than that of an AN copolymer.[10,11] The pres-

ence of the organic solvent CH_3NO_2 in the polymerization medium is not advantageous for formation of PAN nanostructures because they have larger D_n despite their lower D_w/D_n (Table 2). Note that the LPA data were statistically treated by an equivalent-sphere model, and LPA is used here mainly to reveal the size distribution of nanosticks with relatively small aspect ratio. Therefore, exact morphology and size of the nanosticks were determined by TEM.

The morphology of the PAN nanosticks fabricated in the polymerization media of 2 M HNO_3 and 0.5 M H_2SO_4 was observed by TEM (Figure 10). Clearly, the particles look like regular nanosticks with an average diameter of about 40 nm and the length of about 300 nm or longer. The size determined by LPA is different from that by TEM because the LPA data were statistically treated in terms of an equivalent sphere, whereas the PAN nanosticks have an anisotropic shape. Therefore, the size of the PAN nanosticks revealed by TEM is more reliable, but the size distribution (D_w/D_n) revealed by LPA is still significant.

The PAN nanosticks have smooth surfaces without secondary growth. Moreover, the TEM images were obtained on PAN nanostick dispersions that had been stored for half a year after preparation in a yield of up to 80.7%. Apparently, the PAN nanosticks synthesized in this investigation have nearly uniform morphology, superior self-stability, high synthetic yield, and thus potentially extensive applicability.

Why does the chemical oxidative polymerization of AN in 1–2 M HNO_3 aqueous solution afford self-stable nanosticks as products? A possible mechanism of nanostick formation deviating from nanoparticle formation is proposed as follows: When mixed with the HNO_3 solution, AN is first protonated by HNO_3 to form HNO_3–AN salt with hydrophilic/hydrophobic and negatively/positively charged characteristics at the same time. These amphiphilic charged salt could self-assemble into sticklike micelles that act as soft templates for formation of nanosticks (Figure 11). In HNO_3 solution of lower than 1 M concentration, relatively more free neutral ANs would diffuse into the HNO_3–AN micelles, the micelles would become thicker, and finally larger PAN structures would form. On the contrary, when the HNO_3 concentration (1–2 M) is much higher than AN concentration (0.1 M), more ANs would be protonated, and fewer free neutral ANs would be present in the reaction medium. As a result, the number of neutral ANs inside the HNO_3–AN micelles is lower, and the micelles remain thin with high aspect ratio, especially under vigorous stirring. On the dropwise addition of the oxidant solution, these sticklike micelles rapid-

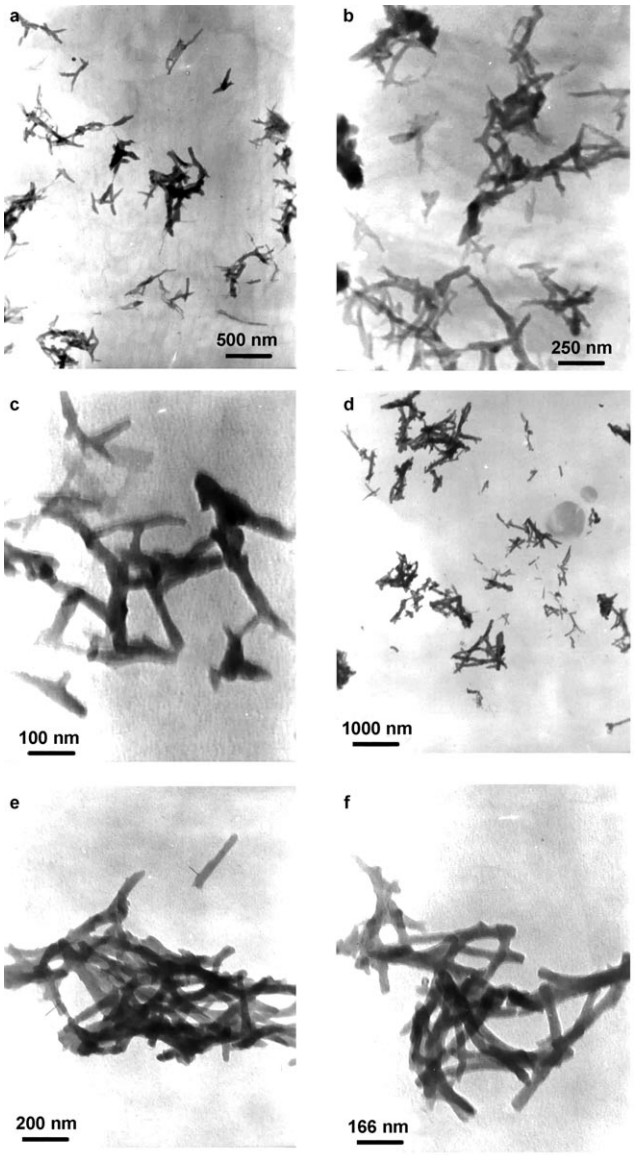

Figure 10. TEM images of PAN nanosticks synthesized in 0.5 M H_2SO_4 (a–c) and 2 M HNO_3 (d–f) with a fixed $(NH_4)_2S_2O_8$/monomer molar ratio of 1/1 at 15 °C for 6 h.

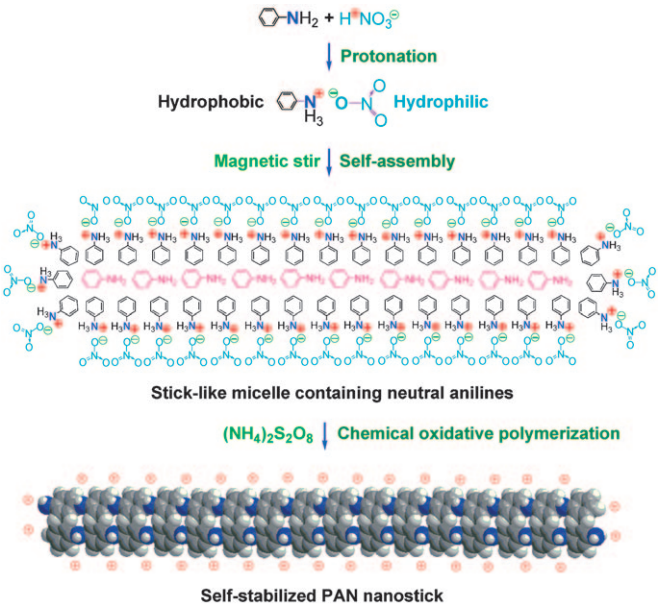

Figure 11. Possible formation mechanism of PAN nanosticks by chemical oxidative polymerization of aniline in 1–2 M HNO_3 aqueous solution with $(NH_4)_2S_2O_8$ as oxidant at a fixed $(NH_4)_2S_2O_8$/aniline molar ratio of 1/1 at 15 °C for 6 h.

ly react with the oxidant to produce positively charged PAN nanosticks in aqueous HNO_3.

Properties of the PAN particles

Bulk electrical conductivity: As shown in Figure 1, the bulk electrical conductivity of the PAN particles increases first and then decreases as the concentration of HNO_3 rises from 0 to 2.5 M.[17] The maximum conductivity of 2.23 $S\,cm^{-1}$ is attained in 2 M HNO_3 as polymerization medium, because the PAN nanosticks obtained in 2 M HNO_3 have maximal π conjugation. Although the doping level would probably be higher in an acid medium of higher concentration than 2 M, the lower conductivity of PAN particles formed in 2.5 M HNO_3 can be attributed to the following reasons: 1) interruption of the long π-conjugated chains by the strong oxidizing power of highly concentrated HNO_3; 2) possible changes in PAN chain structure due to different polymerization mechanisms, including side reactions in concentrated HNO_3 as polymerization medium. For example, PANs obtained by polymerization of AN in very concentrated acid include some -N=N- besides C_{Ar}–N(H)–C_{Ar} linkages, and reactions between AN and HNO_3 involving nitro substitution on phenylene rings and even formation of amino/imino groups are possible.

Moreover, the conductivity of the PAN particles gradually rises on changing the acid medium in the order $H_2O < H_2SO_4 < HCl < HNO_3$ (Table 1). The lowest conductivity of the PAN particles formed in acid-free water must be ascribed to the lowest doping level (Figure 1) and the presence of a small amount of -N=N- linkages (Figure 6), while PAN synthesized in 1 M HNO_3 has the highest conductivity of up to 1.53 $S\,cm^{-1}$ among the three kinds of PAN particles prepared in acid media. In other words, the anionic groups introduced during the polymerization in acid media have a major influence on the conjugated structure and thus conductivity. Adding CH_3NO_2 to the HNO_3 medium leads to PAN particles of lower conductivity (Table 2), and the conductivity is much lower when $FeCl_3$ is used as oxidant rather than $(NH_4)_2S_2O_8$, that is, $FeCl_3$ is not a good oxidant for obtaining electrically conducting PAN particles.

It is important that the PAN nanosticks exhibit stable conductivity. Figure 1 shows that PAN nanosticks stored for 480 d under air at room temperature have only slightly lower conductivity than as-prepared PAN nanosticks, that is, long-term stability of the conductivity is good. As shown in Figure 12, the fact that the conductivity of two types of PAN nanosticks hardly varies with thermal treatment time at 48 °C implies excellent short-term stability of the conductivity. In other words, dedoping of the PAN nanosticks with time in air from ambient temperature to 48 °C is very slow. This is due to strong interaction between the PAN chains and HNO_3 dopant.

Stability of the PAN particles in pure water: The stability of the dispersion of as-prepared PAN particles in water depends on the polymerization medium. As shown in

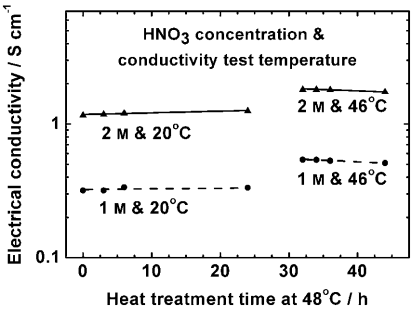

Figure 12. Influence of the heat-treatment time at 48 °C on the bulk electrical conductivity of the 480-day-old sample of PAN nanosticks synthesized with a fixed $(NH_4)_2S_2O_8$/monomer molar ratio of 1/1 at 15 °C for 6 h at HNO_3 concentrations of 1 and 2 M and temperatures of 20 °C and 46 °C.

Figure 13, the three samples synthesized in 2, 1, and 0.5 M HNO_3 exhibit quite different stabilities after standing for 16 h at room temperature. The uniform dispersion of PAN

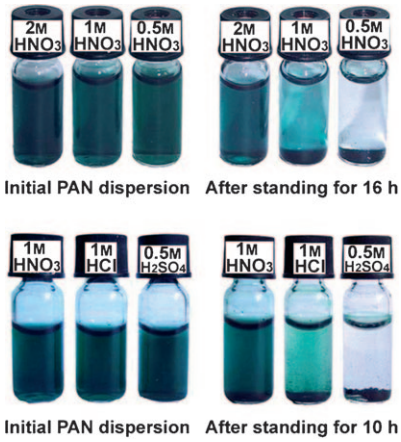

Figure 13. Stability of aqueous dispersions of PAN nanosticks prepared in HNO_3 medium with three concentrations (top) and three acidic media at room temperature (bottom).

nanosticks synthesized in 2 M HNO_3 appears to be stable for several days without aggregation. Clearly, the higher acid concentration is favorable for formation of a uniform dispersion of PAN particles with higher self-stability. This is further evidence that PAN nanosticks with the smallest D_n are obtained in the most concentrated acid (Figure 8). Dependence of stability on doping acid is also illustrated in Figure 13. The aqueous dispersion of PAN nanosticks formed in 1 M HNO_3 has the highest stability after standing for 10 h, and that formed in 0.5 M H_2SO_4 the lowest. These difference in stability can be explained by the different repulsive electrostatic interactions generated by the NO_3^-, Cl^-, and SO_4^{2-} anions that are introduced into the polymer chains by the doping process. Adding electrolyte is another way to influence the stability of the PAN dispersion and confirm the applicability of the electrostatic repulsion theory to this case. The PAN nanosticks synthesized in 2 M

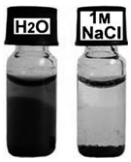

Figure 14. Status of dispersions of the same concentration of PAN nanosticks in water at pH 2.6 (left) and 1 M NaCl (right) after standing for 20 h at 15 °C.

HNO_3 were well dispersed in distilled water at the optimal pH of 2.6[29] and in 1 M NaCl solution. However, the dispersion of PAN nanosticks in water is still stable after standing for 20 h at 15 °C, but the 1 M NaCl electrolyte remarkably lowers the dispersion stability and then accelerates precipitation of the PAN nanosticks (Figure 14). Although the PAN nanosticks flocculate in 1 M NaCl, the precipitated PAN nanosticks are still redispersible by ultrasonic treatment for about 3 min.

Nanocomposite films of PAN nanosticks in PVA matrix: The electrical conductivity of nanocomposite films containing the PAN nanosticks first increases sharply and then slowly with increasing content of PAN nanosticks (Figure 15). The intersection of the two tangents gives the

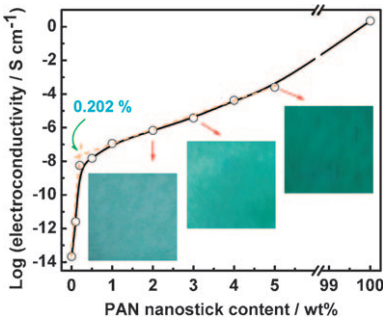

Figure 15. Effect of PAN nanostick content on the electrical conductivity of PAN nanosticks/PVA nanocomposite films. The insets are the photographs of the nanocomposite films containing of 2, 3, and 5 wt % of PAN nanosticks in PVA matrix.

critical concentration that can induce the percolation phenomenon. The determined value of about 0.202 wt % is comparable with that in the nanocomposite based on multiwalled carbon nanotubes.[30] In accordance with percolation theory, when the content of PAN nanosticks exceeds the percolation threshold, their state in the composite film undergoes a transition from the isolated dispersed state to that of contact and connectivity, and finally the conductive network is formed. Accordingly, the nanocomposite film changes from insulator to electrical semiconductor with stable conducting structure. The electrical conductivity reaches a value of up to 2.55×10^{-4} S cm^{-1} at a PAN nanostick content of 5 wt %.[31] This implies that the PAN nanosticks are able to uniformly and stably disperse in viscous polymer solutions or similar media for further practical applicability.[32,33]

Conclusion

Regular PAN nanosticks have been synthesized by facile chemical oxidative polymerization in acidic aqueous media in the absence of any external emulsifier or stabilizer. The polymerization yield, size, polydispersity, morphology, stability, and conductivity of the PAN nanosticks could be significantly optimized by controlling the concentration and nature of the acidic polymerization medium. The optimal polymerization medium for the synthesis of the PAN nanosticks with diameter of about 40 nm, length of about 300 nm, high purity, and high and stable conductivity is an ammonium persulfate/AN molar ratio of 1/1 in 2 M HNO_3 at 15 °C for 6 h, which produces the highest polymerization yield of 80.7 %. Furthermore, the PAN nanosticks are expected to be more suitable for practical application due to their low cost, high yield, facile synthesis, high intrinsic stability, and redispersibility even in viscous media.

Experimental Section

Reagents: Aniline (AN), ammonium persulfate, HNO_3, HCl, H_2SO_4 $BaCl_2$, *N*-methylpyrrolidone (NMP), and poly(vinyl alcohol) (PVA) were of analytical reagent grade and used as received.

Synthesis of PAN nanosticks by chemical oxidative polymerization of AN: A typical procedure for the preparation of nanostructured PAN in 2 M HNO_3 as acidic polymerization medium follows (Scheme 1):[10,11,14,24] Aqueous HNO_3 solution (2.0 M, 80 mL) was added with AN (0.91 mL, 10 mmol) to a 250 mL glass flask in water bath at 15 °C and the mixture stirred vigorously for one hour. Ammonium persulfate (2.28 g, 10 mmol) was dissolved separately in HNO_3 (2.0 M, 20 mL) to prepare an oxidant solution that was kept in the same water bath. The oxidant solution was then added dropwise to the monomer solution at a rate of one drop (60 μL) every 3 s at 15 °C over about 30 min. Then the reaction mixture was continuously stirred for 6 h in a water bath at 15 °C. After the reaction, the virgin HNO_3-doped PAN salts formed were isolated from the reaction mixture by centrifugation and washed with an excess of distilled water to remove residual oxidant and water-soluble oligomers. Ultrasonic dispersion, washing, and centrifugation were repeated three or four times until no SO_4^{2-} was detected by $BaCl_2$ solution. The purified dark green precipitate was divided into two parts, one of which was dispersed in water for direct solution measurements by UV/Vis, TEM, and laser particle-size analysis and direct application for nanocomposite film preparation, and the other left to dry under an infrared lamp at 40 °C for one week for determination of the polymerization yield and FTIR and XRD measurements.

Preparation of the nanocomposite film: The PAN nanosticks were prepared with a fixed $(NH_4)_2S_2O_8$/monomer molar ratio of 1/1 in 2 M HNO_3 at 15 °C for 6 h. Aqueous dispersions of PAN nanosticks (2.5 mL) of different contents were well mixed with an equal volume of 4 % aqueous PVA solution (1 g in 25 mL water) by ultrasonically dispersing for 2.0 h to prepare several groups of composite solutions. Then the composite solution was cast onto a polytetrafluoroethylene plate. After drying in an oven at 35 °C for 24 h, the 10–20 μm-thick film was peeled off the substrate to form a free-standing film for performance evaluation.

Measurements: IR spectra were recorded on KBr pellets on a Nicolet Magna 550 FTIR spectrometer at 2 cm^{-1} resolution. The UV/Vis spectra of PAN particle dispersions in water and PAN solution in NMP were obtained on a Lambda 35 UV/Vis spectrophotometer (Perkin–Elmer Instruments) in the wavelength range of 190–900 nm at a scanning rate of 400 nm min^{-1}. Wide-angle X-ray diffractograms were obtained by using a D/max 2550 model X-ray diffractometer with $Cu_{K\alpha}$ radiation over a 2θ range from 5 to 70°. The size and size distribution of the as-prepared

PAN particles in water were analyzed on a Beckman Coulter LS230 laser particle-size analyzer. The size and morphology of the particles were further observed by a Hitachi model H600 transmission electron microscope. The bulk electrical conductivities of the PAN pellets and nanocomposite films were calculated by measuring the resistance and thickness of the pellets or films between two round-disk stainless steel electrodes with a diameter of 1 cm with a multimeter and a thickness gauge at 20 °C, respectively. The relative error for various measurements is less than 5 %

Acknowledgement

The project is supported by the National Natural Science Fund of China (Grant No. 20774065 and 50773053) and Key Laboratory of Molecular Engineering of Polymers, Fudan University, China.

[1] A. G. MacDiarmid, *Synth. Met.* **2002**, *125*, 11.
[2] D. Li, R. B. Kaner, *J. Am. Chem. Soc.* **2006**, *128*, 968.
[3] L. Zhang, X. E. Jiang, L. Niu, S. J. Dong, *Biosens. Bioelectron.* **2006**, *21*, 1107.
[4] A. G. MacDiarmid, W. E. Jones, I. D. Norris, J. Gao, A. T. Johnson, N. J. Pinto, J. Hone, B. Han, F. K. Ko, H. Okuzaki, M. Llaguno, *Synth. Met.* **2001**, *119*, 27.
[5] H. X. He, C. Z. Li, N. J. Tao, *Appl. Phys. Lett.* **2001**, *78*, 811.
[6] S. L. Mu, *Synth. Met.* **2006**, *156*, 202.
[7] L. X. Zhang, L. J. Zhang, M. X. Wan, Y. Wei, *Synth. Met.* **2006**, *156*, 454.
[8] X. F. Lu, H. Mao, D. M. Chao, W. J. Zhang, Y. Wei, *J. Solid State Chem.* **2006**, *179*, 2609.
[9] Y. J. He, *Appl. Surf. Sci.* **2005**, *249*, 1.
[10] a) X. G. Li, Q. F. Lü, M. R. Huang, *Chem. Eur. J.* **2006**, *12*, 1349; b) Q. F. Lü, M. R. Huang, X. G. Li, *Chem. Eur. J.* **2007**, *13*, 6009; c) X. G. Li, Q. F. Lü, M. R. Huang, *Small* **2008**, *4*, 1201.
[11] X. G. Li, R. R. Zhang, M. R. Huang, *J. Comb. Chem.* **2006**, *8*, 174.
[12] J. X. Huang R. B. Kaner, *J. Am. Chem. Soc.* **2004**, *126*, 851; *Chem. Commun*. **2006**, *4*, 367.
[13] a) L. Yu, J. I. Lee, K. W. Shin, C. E. Park, R. Holze, *J. Appl. Polym. Sci.* **2003**, *88*, 1550; b) E. T. Kang, K. G. Neoh, K. L. Tan, *Prog. Polym. Sci.* **1998**, *23*, 277; c) Y. P. Fu, R. L. Elsenbaumer, *Chem. Mater.* **1994**, *6*, 671; d) K. C. Huang, R. A. Couttenye, G. E. Hoag, *Chemosphere* **2002**, *49*, 413.
[14] X. G. Li, H. Li, M. R. Huang, *Chem. Eur. J.* **2007**, *13*, 8884.
[15] A. B. Samui, A. S. Patankar, R. S. Satpute, P. C. Deb, *Synth. Met.* **2002**, *125*, 423.
[16] J. S. Tang, L. X. Wang, X. B. Jing, B. C. Wang, F. S. Wang, *Acta Polym. Sin.* **1989**, 188.
[17] J. K. Avlyanov, Y. Min, A. G. MacDiarmid, A. J. Epstein, *Synth. Met.* **1995**, *72*, 65.
[18] J. X. Huang, S. Virji, B. H. Weiller, R. B. Kaner, *J. Am. Chem. Soc.* **2003**, *125*, 314.
[19] J. X. Huang, J. A. Moore, J. H. Acquaye, R. B. Kaner, *Macromolecules* **2005**, *38*, 317.
[20] A. Drury, S. Chaure, M. K. V. Nicolosi, N. Chaure, W. J. Blau, *Chem. Mater.* **2007**, *19*, 4252.
[21] H. Zengin, W. Zhou, J. Jin, R. Czerw, D. W. Smith Jr. , L. Echegoyen, D. L. Carroll, S. H. Foulger, J. Ballato, *Adv. Mater.* **2002**, *14*, 1480.
[22] H. Liu, X. B. Hu, J. Y. Wang, R. I. Boughton, *Macromolecules* **2002**, *35*, 9414.
[23] a) S. Quillard, G. Louarn, S. Lefrant, A. G. MacDiarmid, *Phys. Rev. B* **1994**, *50*, 12496; b) T. Ohsaka, Y. Ohnuki, N. Oyama, G. Katagiri, K. Kamisako, *J. Electroanal. Chem.* **1984**, *161*, 399.
[24] X. G. Li, M. R. Huang, Y. Q. Lu, M. F. Zhu, *J. Mater. Chem.* **2005**, *15*, 1343.
[25] J. P. Pouget, M. E. Jozefowicz, A. J. Epstein, X. Tang, A. G. MacDiarmid, *Macromolecules* **1991**, *24*, 779.
[26] M. L. Singla, S. Awasthi, A. Srivastava, D. V. S. Jain, *Sens. Actuators A* **2007**, *136*, 604.
[27] Y. B. Moon, Y. Cao, P. Smith, A. J. Heeger, *Polym. Commun.* **1989**, *30*, 196.
[28] J. P. Pouget, C. H. Hsu, A. G. MacDiarmid, A. J. Epstein, *Synth. Met.* **1995**, *69*, 119.
[29] D. Li, R. B. Kaner, *Chem. Commun.* **2005**, 32.
[30] S. T. Kim, H. J. Choi, S. M. Hong, *Colloid Polym. Sci.* **2007**, *285*, 593.
[31] W. Prissanaroon, L. Ruangchuay, A. Sirivat, J. Schwank, *Synth. Met.* **2000**, *114*, 65.
[32] M. S. Cho, H. J. Choi, W. S. Ahn, *Langmuir* **2004**, *20*, 202.
[33] M. S. Cho, S. Y. Park, J. Y. Hwang, H. J. Choi, *Mater. Sci. Eng. C* **2004**, *24*, 15.

Received: May 28, 2008
Revised: August 1, 2008
Published online: October 1, 2008

